chemosensors

MDPI

Supporting Information

Dual Transduction of H_2O_2 Detection Using ZnO/Laser-Induced Graphene Composites

Julia Zanoni [1], Jorge P. Moura [1], Nuno F. Santos [1], Alexandre F. Carvalho [1,2], António J. S. Fernandes [1], Teresa Monteiro [1], Florinda M. Costa [1], Sónia O. Pereira [1] and Joana Rodrigues [1,*]

[1] i3N, Department of Physics, University of Aveiro, 3810-193 Aveiro, Portugal; julia.ines@ua.pt (J.Z.); jorgemoura@ua.pt (J.P.M.); nfsantos@ua.pt (N.F.S.); alexandre.carvalho@ua.pt (A.F.C.); toze2@ua.pt (A.J.S.F.); tita@ua.pt (T.M.); flor@ua.pt (F.M.C.); sonia.pereira@ua.pt (S.O.P.)
[2] CICECO—Aveiro Institute of Materials, Department of Physics, University of Aveiro, 3810-193 Aveiro, Portugal
* Corresponding author: joana.catarina@ua.pt

1. Experimental Details

1.1. Samples

Table S1. Summary of the growth/synthesis condition employed for both materials comprising the ZnO/LIG composites.

Materials	Growth/Synthesis parameters	
LIG	Laser wavelength	10.6 µm
	Laser power	~ 12 W
	Scan speed	250 mm s^{-1}
	Distance between scanning lines	0.075 mm
	Distance to focus	~ 1.8 mm
	Atmosphere	air
ZnO	Laser wavelength	10.6 µm
	Laser power	~ 60 W
	Atmosphere	air

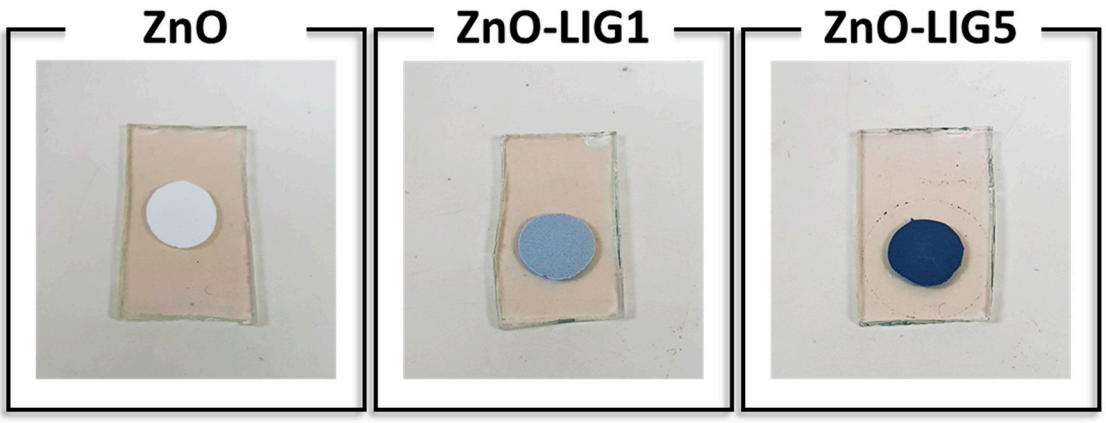

Figure S1. Pictures of the produced samples that were obtained after the thermal treatment.

1.2. Experimental Characterization Setup

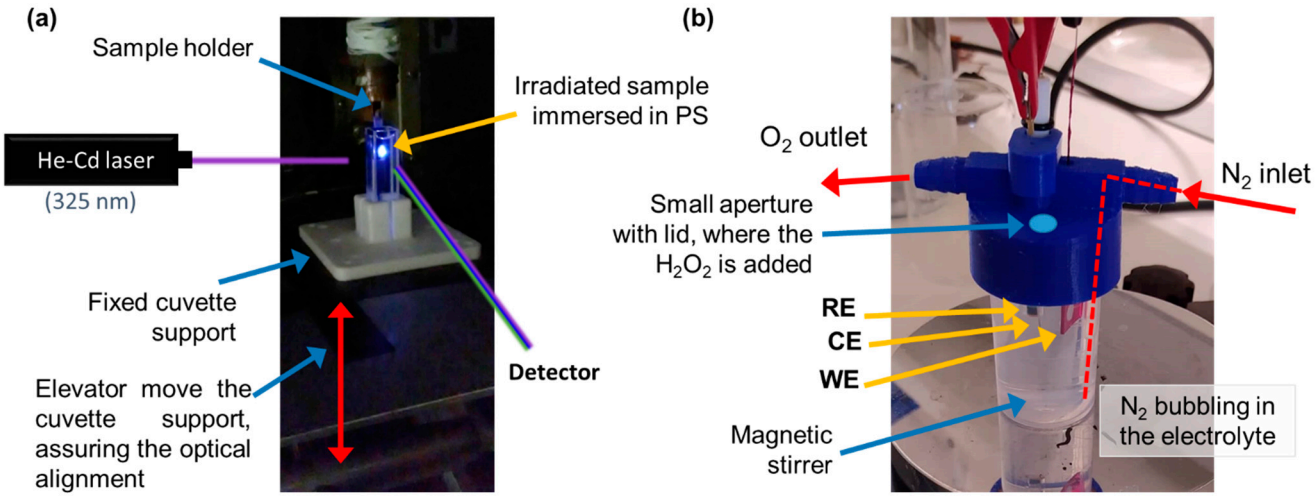

Figure S2. (**a**) PL and (**b**) electrochemical experimental setups used for the assessment of H_2O_2 detection.

2. Photoluminescence Characterization

2.1. Temperature-Dependent PL

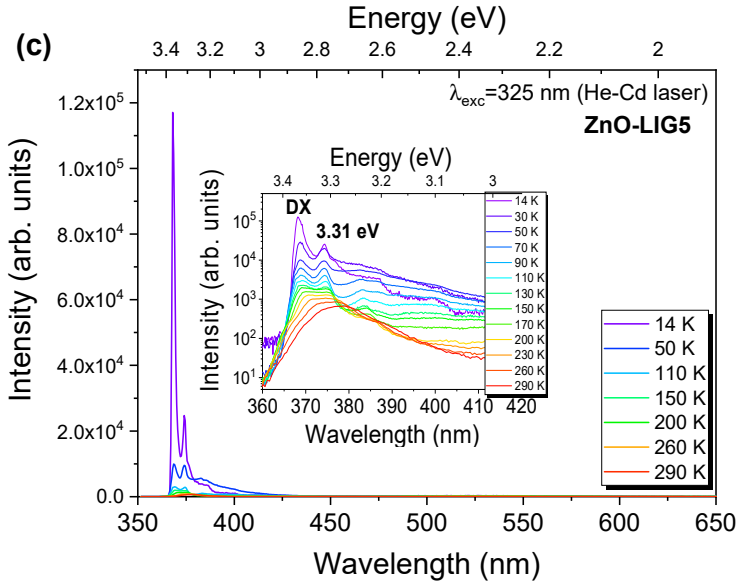

Figure S3. Temperature dependence PL recorded in the UV-visible range for the samples: (**a**) ZnO, (**b**) ZnO-LIG1 and (**c**) ZnO-LIG5. The samples were excited with the 325 nm line of a He-Cd laser. The insets correspond to a magnification of the UV spectral region, showing a higher range of temperatures.

3. Electrochemical Characterization

3.1. Scan Rate Dependence Study

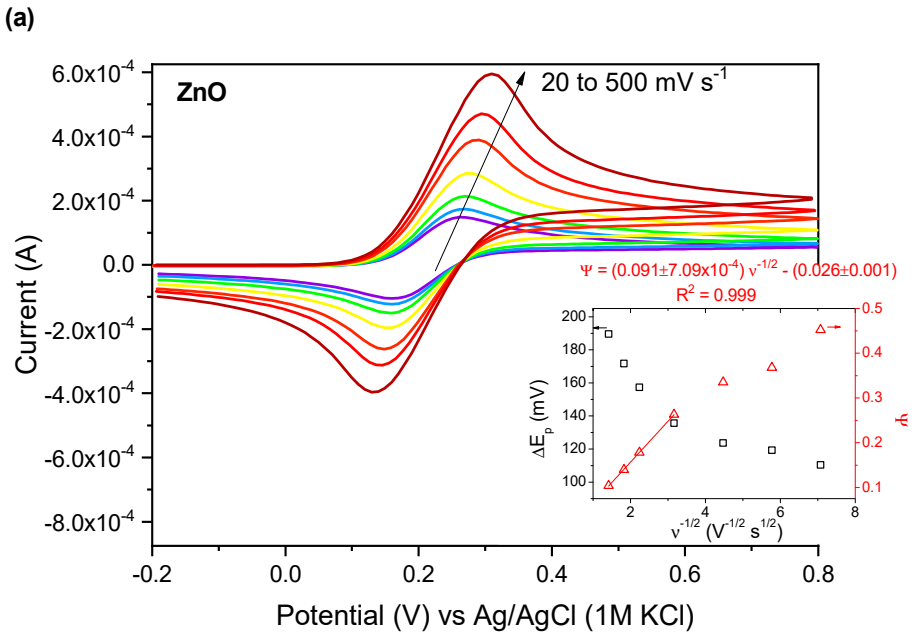

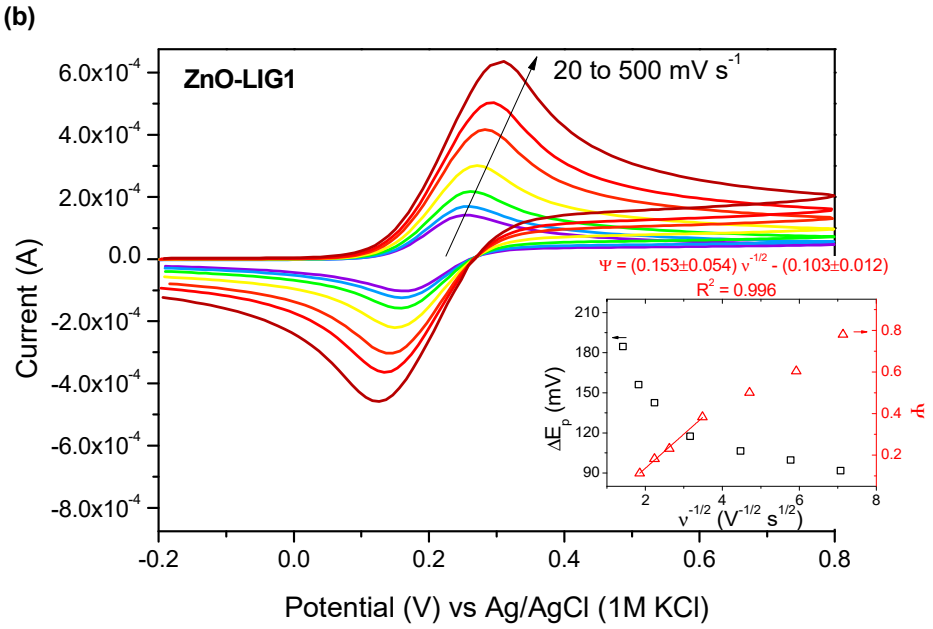

Figure S4. Cyclic voltammograms at different scan rates, from 20 to 500 mV s^{-1}, of representative samples of (**a**) ZnO and (**b**) ZnO-LIG1 using 10 mM of $[Fe(CN)_6]^{4-}$ in PS as the electrolyte. Inset: Corresponding plot of ΔE_p and Ψ parameter against $v^{-1/2}$.

4. Effect of Immersion in Physiological Solution

4.2 Photoluminescence Monitoring

Error! Reference source not found. shows how the PL signal of both ZnO and ZnO-LIG5 samples is affected when immersed in the PS. It was observed that after 5 min of immersion in PS, a strong reduction of the PL intensity, together with a change in the relative intensities of the UV and GL emissions were identified, which can be explained by the occurrence of dissociative adsorption of water molecules at the surface of the semiconductor, as reported by other authors [1–5]. This means that OH groups will be formed on the ZnO surface, leading to a hydroxylated surface, which is then easily wet by water [1,2]. Afterwards, water molecules interact with those groups and water adlayers on the OH–ZnO surface are formed by continuous exposure to water [1]. Several studies indicate that the way water interacts with the ZnO surface depends on the orientation of the ZnO surface planes and the defects present at the surface [1–3,5]. For instance, oxygen vacancies seem to be preferential binding sites for the water dissociation and attachment of the OH-species, while the H atoms adsorbed on the surface become rather mobile and diffuse [1,3]. As mentioned, the presence of these OH-species at the surface of ZnO will generate an additional charge density at the surface, therefore affecting the bending of the electronic energy bands at the semiconductor/water interface (see a schematic illustration in **Error! Reference source not found.**). As a n-type semiconductor, increasing the negative charge density at the ZnO surface will conduct to a further upward band bending, thus increasing the potential barrier that the carriers have to overcome to recombine radiatively [6,7]. Subsequently, quenching in the PL intensity is observed, especially for the bulk-related transitions, as for the FX recombination that dominates the PL spectra at RT. This is indeed what was observed in the present samples after being immersed in the PS (scheme (ii) in Figure S6a). After this process, a second tendency is observed in a reproducible way: for the ZnO samples a progressive enhancement in the PL intensity is observed with increasing time in the solution during UV irradiation, resulting in signal stabilization after ~2.5 h (**Error! Reference source not found.**a); whereas, for the case of the ZnO/LIG composite, the intensity of the PL signal increases only slightly with the immersion time under

UV irradiation (**Error! Reference source not found.**b). The signal was seen to be much more stable than in the case of ZnO, needing only ~30-45 min for that stabilization.

The final reduction of the signal for the ZnO-LIG5 sample was nearly 3 times the initial one, contrasting with the ~1.4 times observed for ZnO. This quenching was particularly evident in the UV region, with the GL/UV peak intensity ratio increasing from ~0.27 to ~0.48 in the case of the composite (~0.37 to ~0.34 for ZnO), which was barely affected by the continuous UV irradiation.

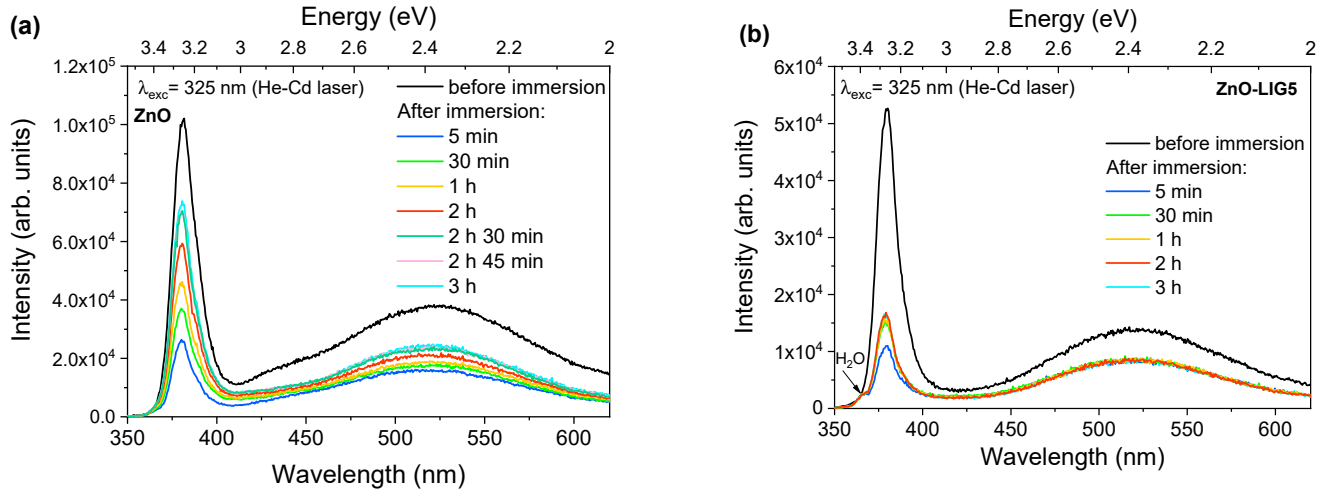

Figure S5. Representative PL spectra obtained for the (**a**) ZnO and (**b**) ZnO-LIG5 before and after their immersion into the physiological solution (from 5 min to 3 h) under UV illumination (325 nm, He-Cd laser).

These findings indicate that the band bending dynamics is strongly sensitive to above bandgap energy irradiation and the initial characteristics of the surface. For ZnO, the UV illumination results in the charging of the surface by the photogenerated pairs, which decreases the surface potential barrier. Therefore, this reduces the band bending (scheme (iii) in **Error! Reference source not found.**a) [7], enhancing the radiative recombination of the photogenerated carriers. However, in the case of the ZnO mixed with LIG, the radiative recombination of the photogenerated electron-hole pairs in ZnO is inhibited. This means that contrarily to the bare ZnO samples, for the ZnO/LIG only a small reduction of the band bending occurs after illumination (scheme (iii) in **Error! Reference source not found.**b), which means that a distinct ZnO surface charge was promoted upon irradiation, induced by the presence of the LIG. The experimental observations suggest that the photogenerated carriers are likely to be preferentially captured by the LIG material owning to its higher photon absorption capability [8], as mentioned in the main text. Unlike the dry case, the charge transfer to the electron-hole pairs to ZnO seems to be hindered in the presence of water, thus not contributing to the decrease in the surface potential as inferred for ZnO.

This effect on the increase of the PL signal under continuous UV irradiation was seen to be more pronounced in the case of the NBE recombination, indicating that the defect-related emission, namely the one associated with the surface defects that participate in the GL emission, is less affected by these phenomena. Indeed, the increase in the band bending tends to benefit the surface recombination over the bulk one [6], thus the excitonic-related emission is the one that suffers more pronounced variations with the band bending reduction.

Although this discussion was made solely based on the water interaction with the ZnO surface, it is important to bear in mind that the presence of the PS salts may also play

a role in this process, also influencing the charge density at the surface of the semiconductor.

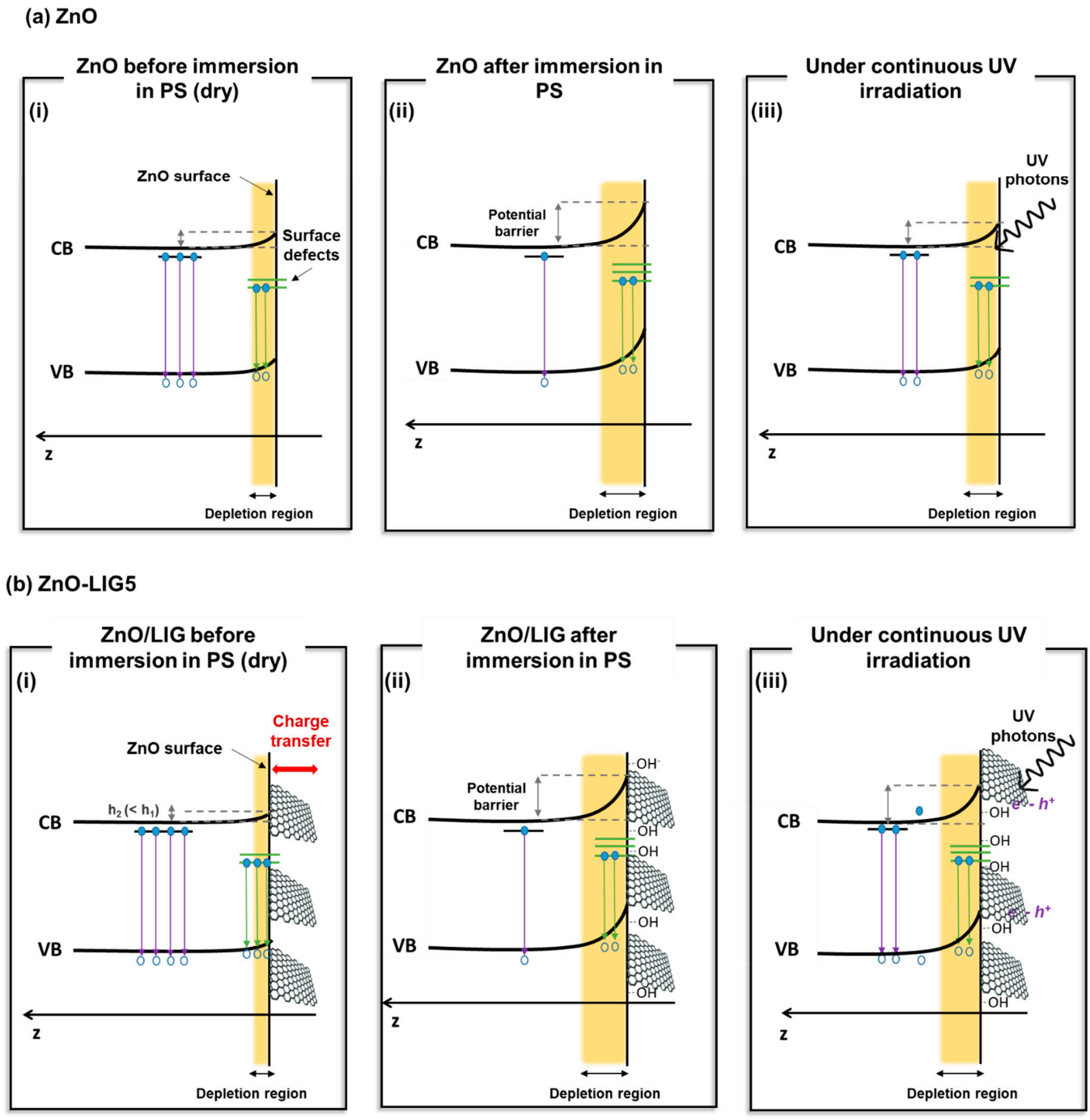

Figure S6. Schematic diagram illustrating the effect of the immersion of the samples in the PS solution and subsequent continuous UV irradiation: (a) ZnO and (b) ZnO-LIG5 (representative for ZnO/LIG composites; for clarity, functional groups of LIG are not displayed in the simplified representation of LIG). The straight arrows denote radiative recombination processes. h_1 and h_2 correspond to the heights of the potential barrier for ZnO and ZnO-LIG5, respectively. The full circles represent electrons, while the open ones correspond to holes.

5. H_2O_2 Sensing

5.1. Via Photoluminescence Monitoring

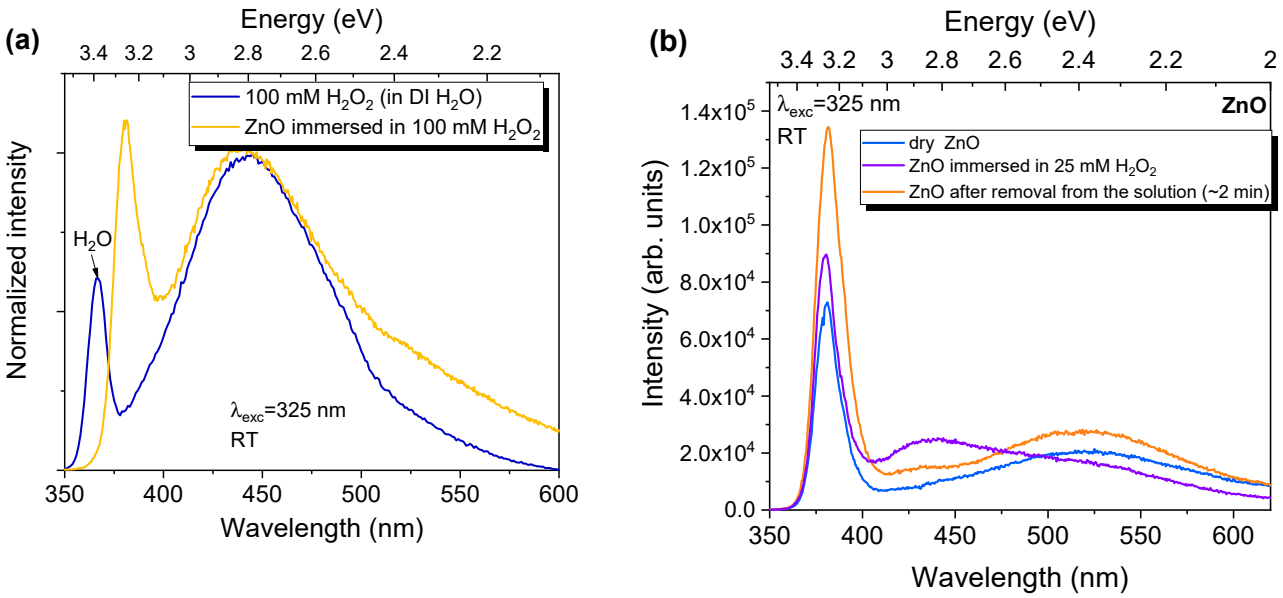

Figure S7. (**a**) Comparison between the PL signal of 100 mM of H_2O_2 (in DI water) and the one of the ZnO sample immersed in a similar solution. (**b**) PL spectra of a ZnO sample before, during and after its immersion in a 25 mM of H_2O_2 solution (in DI water).

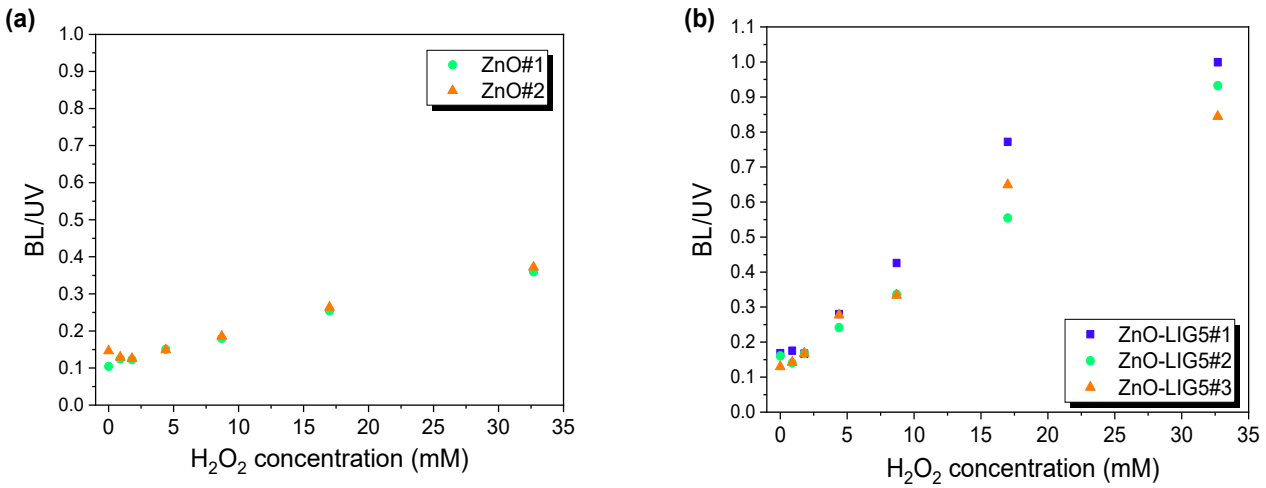

Figure S8. Peak intensity ratio BL/UV (measured at 438 nm and 380 nm, respectively) as a function of the H_2O_2 concentration for the tested (a) ZnO and (b) ZnO-LIG5 samples.

5.2. Via Electrochemical Monitoring

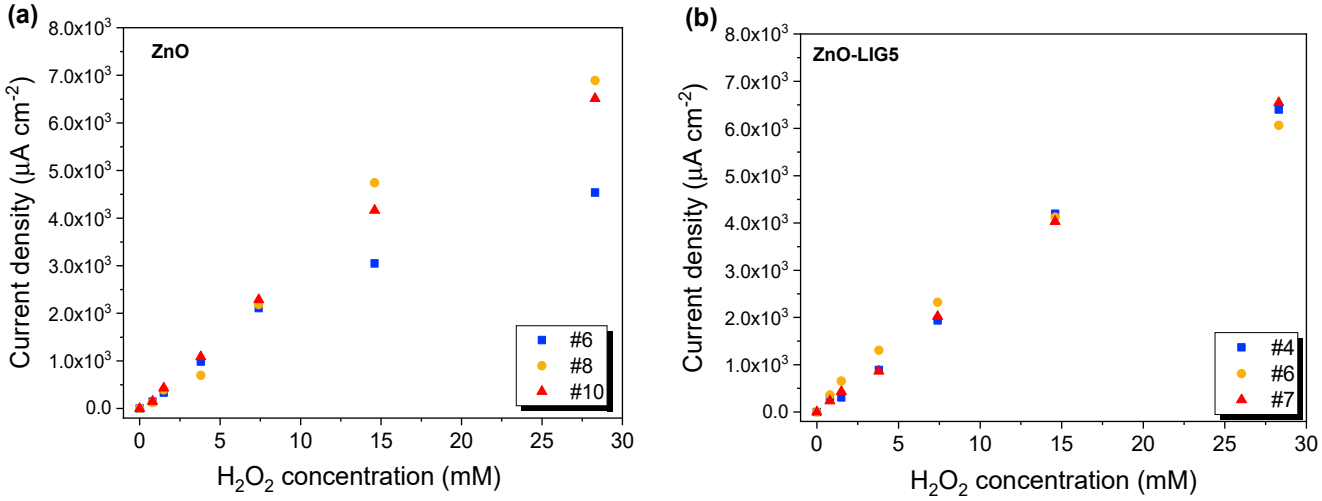

Figure S9. Current density at the peak maxima (located at ~0.5 - 0.6 V) as a function of the H_2O_2 concentration obtained for the three replicas of (a) ZnO and (b) ZnO-LIG5 samples.

References

1. Wöll, C. The chemistry and physics of zinc oxide surfaces. *Prog. Surf. Sci.* **2007**, *82*, 55–120, doi:10.1016/j.progsurf.2006.12.002.
2. Wang, Y.; Muhler, M.; Wöll, C. Spectroscopic evidence for the partial dissociation of H_2O on ZnO($10\bar{1}0$). *Phys. Chem. Chem. Phys.* **2006**, *8*, 1521, doi:10.1039/b515489h.
3. Kunat, M.; Girol, S.G.; Burghaus, U.; Wöll, C. The Interaction of Water with the Oxygen-Terminated, Polar Surface of ZnO. *J. Phys. Chem. B* **2003**, *107*, 14350–14356, doi:10.1021/jp030675z.
4. Hu, H.; Ji, H.-F.; Sun, Y. The effect of oxygen vacancies on water wettability of a ZnO surface. *Phys. Chem. Chem. Phys.* **2013**, *15*, 16557, doi:10.1039/c3cp51848e.
5. Dulub, O.; Meyer, B.; Diebold, U. Observation of the Dynamical Change in a Water Monolayer Adsorbed on a ZnO Surface. *Phys. Rev. Lett.* **2005**, *95*, 136101, doi:10.1103/PhysRevLett.95.136101.
6. Rodrigues, J.; Ben Sedrine, N.; Correia, M.R.; Monteiro, T. Photoluminescence investigations of ZnO micro/nanostructures. *Mater. Today Chem.* **2020**, *16*, 100243, doi:10.1016/j.mtchem.2020.100243.
7. Stevanovic, A.; Büttner, M.; Zhang, Z.; Yates, J.T. Photoluminescence of TiO_2 : Effect of UV Light and Adsorbed Molecules on Surface Band Structure. *J. Am. Chem. Soc.* **2012**, *134*, 324–332, doi:10.1021/ja2072737.
8. Bao, Q.; Zhang, H.; Wang, Y.; Ni, Z.; Yan, Y.; Shen, Z.X.; Loh, K.P.; Tang, D.Y. Atomic-Layer Graphene as a Saturable Absorber for Ultrafast Pulsed Lasers. *Adv. Funct. Mater.* **2009**, *19*, 3077–3083, doi:10.1002/adfm.200901007.